Supplementary Materials and Methods

Aspergillus fumigatus strain and preparation of hyphae

A. fumigatus strain CCTCC 93024 was purchased from the China Centre for Type Culture Collection and cultured on Sabouraud dextrose agar (213400, BD Bioscience, Franklin Lakes, NJ, USA) in an incubator for 7 days at 37°C. Hyphal fragments and conidia were harvested and planted into Sabouraud fluid media, and shaken at 26 °C for 18 h at 500 rpm. Next, the tubes were centrifuged at 1500 g for 10 min. For the in vitro study, the mycelia were washed twice and then suspended in PBS, followed by heat-inactivation at 56 °C for 60 min. They were then disrupted into 20- to 40-μm pieces with a tissue grinder and used at a density of 1×10^6 pieces/mL. For the in vivo study, conidia and hyphae were diluted in phosphate-buffered saline (PBS) into 2×10^8 pieces/mL and used at a density of 1×10^8 pieces/mL.

RNA interference

Specific siRNA oligonucleotides and negative control (NC) siRNA were designed and synthesized by GenePharma (Shanghai, China). The siRNA sequence pools targeting the coding region of TSLP and TSLPR are shown in the supplementary information. For the in vitro study, cells were seeded at 2×10^5 cells/well in six-well plates in a normal growth medium; next, they were transfected with either 80 nm siRNA or NC siRNA for 48 h using Lipofectamine 2000 reagent (11668-019, Invitrogen, Waltham, MA, USA) following the manufacturer's recommendations. The gene silencing efficiency was verified by qRT-PCR and western blot. For the in vivo study, mice were anesthetized as previously described. TSLP siRNA or NC siRNA were diluted in sterile water to a

concentration of 10 μmol/L each. One day before *A. fumigatus* infection, the mice were subconjunctivally injected with 5 μL of either TSLP siRNA or NC siRNA.

Immunofluorescence Staining

Eyeballs were excised from euthanized mice and embedded into the optimal cutting temperature (OCT) compound (Sakura, Torrance, CA, USA). Sections were cut into 6-μm thick slices, mounted on polylysine-coated glass slides, fixed in 4% paraformaldehyde for 20 min, and then blocked with 2% bovine serum albumin (BSA) for 1 h at RT. Subsequently, slides were incubated with the primary antibody (1:100) overnight at 4 °C, and then incubated with the corresponding secondary antibody conjugated to FITC or TRITC (1:200, Beyotime) for 1 h at RT. The nuclei were counterstained with DAPI for 5 min in the dark. For the in vitro assay, cells were fixed with 4% paraformaldehyde for 15 min and blocked with 5% BSA for 1 h at RT; next, they were incubated with CD11c and TSLP antibodies, corresponding secondary antibody, and DAPI. Finally, slides were covered with antifade mounting medium and coverslips. Images were collected by fluorescence microscopy (X81, Olympus Optical, Tokyo, Japan).

High-throughput differential gene expression analysis

The high-throughput mRNA-Seq experiments were conducted and analyzed by Biomarker Technologies (Beijing, China).

Supplementary Figures:

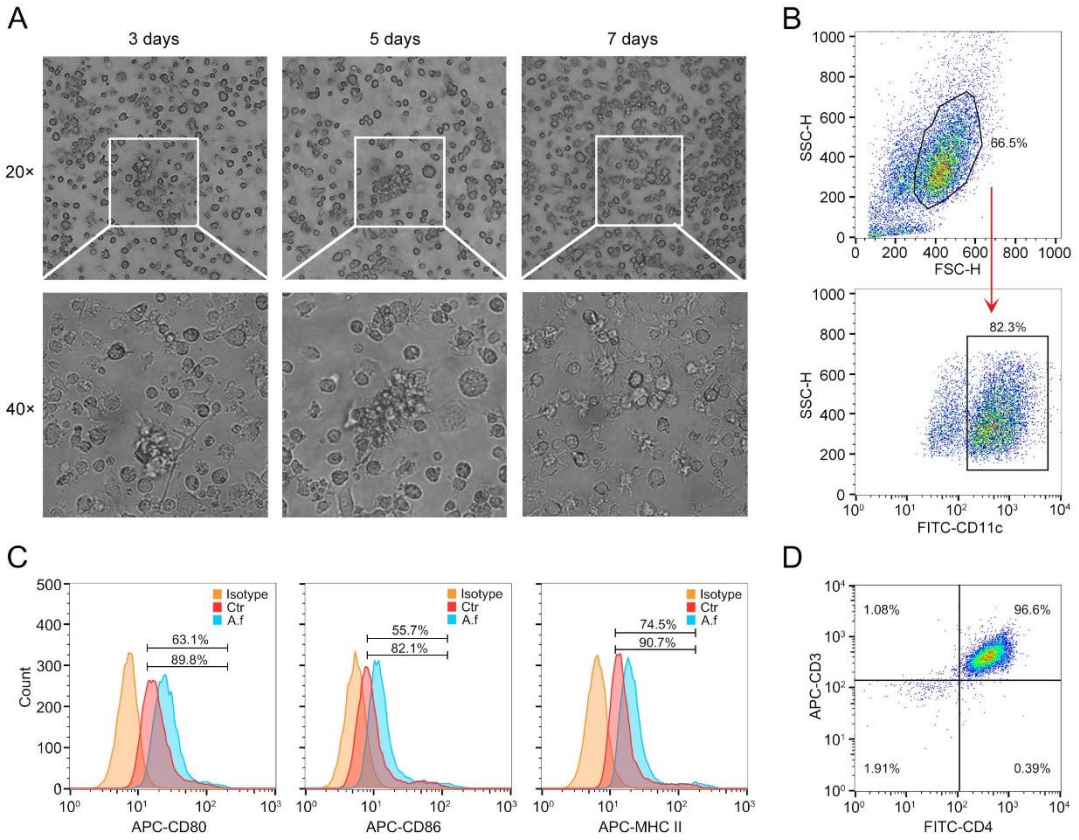

Figure S1. Identification of the morphology and concentration of DCs and $CD4^+$T cells. (A) Images of the DCs cultured at day 3, 5, and 7 showing the increase in cell number and change in cell morphology. The under panel are digitally magnified images of cells in this fraction with dendritic morphology. (B) Flow cytometry was performed to examine the surface expression of CD11c in DCs at the 5th day. Gating straight for flow cytometry was also shown. (C) DCs were cultured for 5 days, stimulated with *A. fumigatus* hyphae (10^6 pieces/mL) for 12 h. The surface expression of CD80, CD86, and MHC-II in $CD11c^+$ DCs was detected using flow cytometry. (D) Isolated $CD4^+$ T cells were stained with FITC-CD4 and APC-CD3, flow cytometry was performed to detect the surface expression of CD4 and CD3.

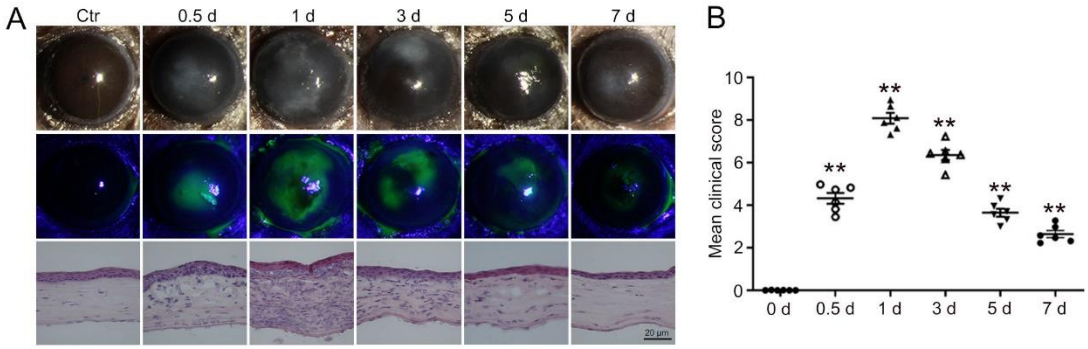

Figure S2. C57BL/6 mice corneas were scratched with 26-gauge needles followed by treatment with *A. fumigatus* for 0.5, 1, 3, 5, and 7 days. (A) The severities of keratitis were assessed by slit-lamp examination, fluorescein staining, and H&E staining at 0.5, 1, 3, 5, and 7 days post-infection. Scale bar: 20 μM. (B) Clinical scores were calculated to assess the clinical manifestation in (A). (Data are mean ± SEM, *$p < 0.05$, **$p < 0.01$, n = 6).

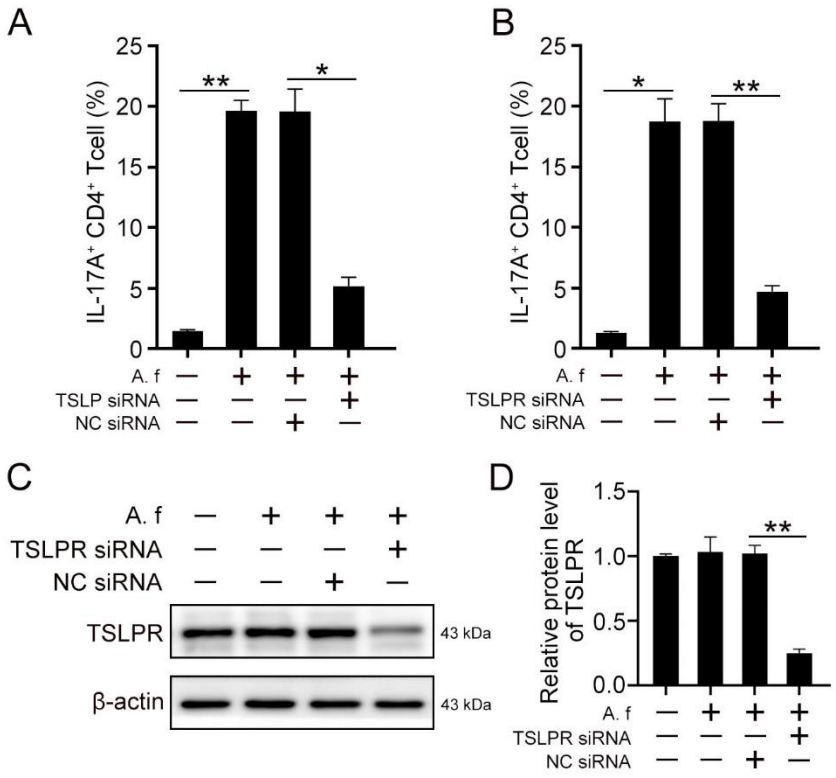

Figure S3. (A) Quantification of IL-17A level in Figure 4F. (B) Quantification of IL-17A level in Figure 4H. (C) $CD4^+$ T cells were incubated with TLSPR siRNA (80 nM) or NC siRNA for 24 h, then co-cultured with *A. fumigatus*-stimulated DCs for 4 days. Western blot was performed to detect the protein levels of IL-17A and β-actin in $CD4^+$ T cells. (D) Quantification of TSLPR level in (C). (Data are mean ± SEM, $*p < 0.05$, $**p < 0.01$, n = 3).

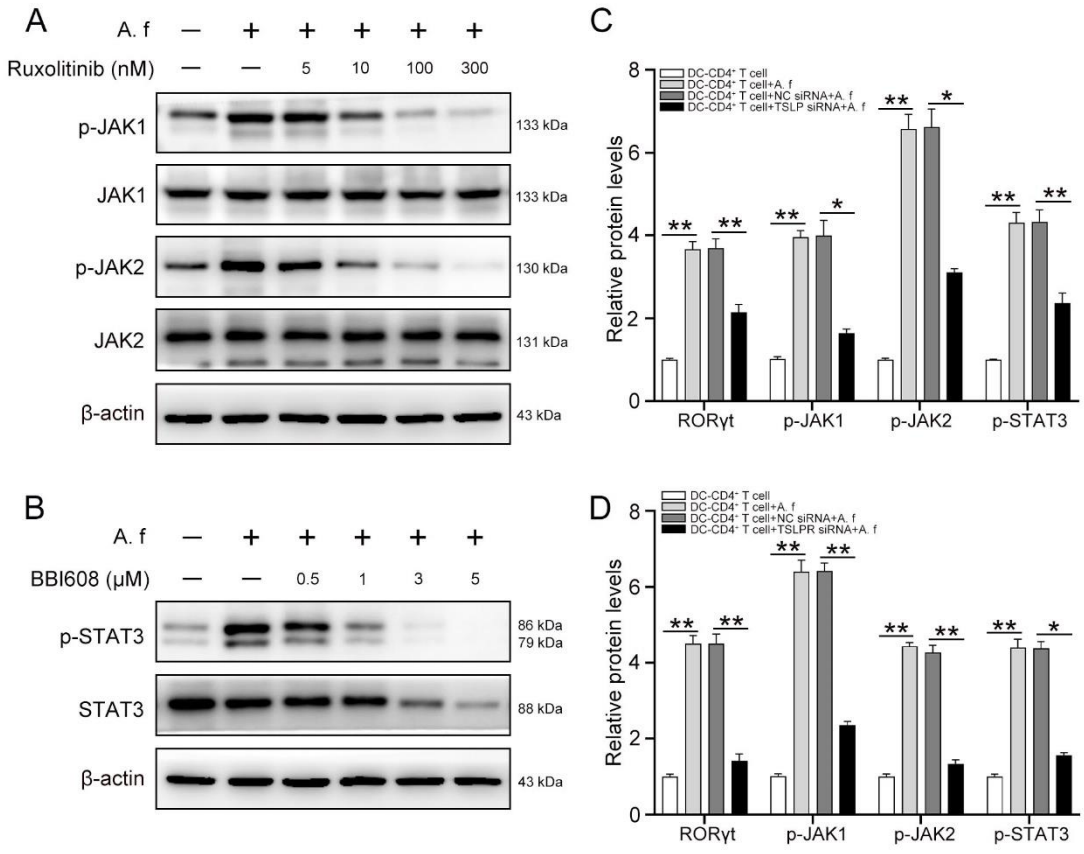

Figure S4. $CD4^+$ T cells co-cultured with *A. fumigatus*-stimulated DCs were treated with different concentration of ruxolitinib (5, 10, 100, and 300 nM) or BBI608 (0.5, 1, 3, and 5 μM) for 4 days. (A) Western blot was performed to determine the protein levels of p-JAK1, JAK1, p-JAK2, JAK2, and β-actin in $CD4^+$ T cells. (B) Western blot was performed to determine the protein levels of p-STAT3, STAT3, and β-actin in $CD4^+$ T

cells. (C) Quantification of relative protein levels of p-STAT3, p-JAK1, p-JAK2, and RORγt in Figure 6E. (D) Quantification of relative protein levels of p-STAT3, p-JAK1, p-JAK2, and RORγt in Figure 6F. (Data are mean ± SEM, *$p < 0.05$, **$p < 0.01$, n = 3).

Table S1. siRNA sequences used for RNA interference and Primer sequences used for qRT-PCR

Gene	**siRNA sequences (5' to 3')**
TSLP-1	CACAAGAAGUCCAAAACAU
TSLP-2	GGGAGAAACUGCUGAGAUC
TSLP-3	CCUCACAAAUUCUAAGAUU
TSLPR-1	GGACCGAACCAGCUGUCAAUC
TSLPR-2	GGACCGAGGAGGAAGAUGACC
TSLPR-3	GCAAAUGUGGUCACAAAUAUU
Gene	**Primer sequences (5' to 3')**
GADPH-F	CATCACTGCCACCCAGAAGACTG
GADPH-R	ATGCCAGTGAGCTTCCCGTTCAG
TSLP-F	GCAAATCGAGGACTGTGAGAGC
TSLP-R	TGAGGGCTTCTCTTGTTCTCCG
IL-6-F	TACCACTTCACAAGTCGGAGGC
IL-6-R	CTGCAAGTGCATCATCGTTGTTC

IL-23-F	CATGCTAGCCTGGAACGCACAT
IL-23-R	ACTGGCTGTTGTCCTTGAGTCC
IL-1β-F	CCTTCCAGGATGAGGACATGA
IL-1β-R	TGAGTCACAGAGGATGGGCTC
IL-17A-F	CAGACTACCTCAACCGTTCCAC
IL-17A-R	TCCAGCTTTCCCTCCGCATTGA
IL-17F-F	AACCAGGGCATTTCTGTCCCAC
IL-17F-R	GGCATTGATGCAGCCTGAGTGT
IL-22-F	GCTTGAGGTGTCCAACTTCCAG
IL-22-R	ACTCCTCGGAACAGTTTCTCCC
Bcl2-F	CCTGTGGATGACTGAGTACCTG
Bcl2-R	AGCCAGGAGAAATCAAACAGAGG
Bcl2l1-F	GCCACCTATCTGAATGACCACC
Bcl2l1-R	AGGAACCAGCGGTTGAAGCGC
Socs3-F	GGACCAAGAACCTACGCATCCA
Socs3-R	CACCAGCTTGAGTACACAGTCG
Socs1-F	AGTCGCCAACGGAACTGCTTCT
Socs1-R	GTAGTGCTCCAGCAGCTCGAAA
Il21r-F	CACTGACTACCTCTGGACCATC
Il21r-R	GCAGAAGGTCTCTTGGTCCTGA
Stat5a-F	CCTGTTTGAGTCTCAGTTCAGCG

Stat5a-R	TGGCAGTAGCATTGTGGTCCTG
Lif-F	TCAACTGGCACAGCTCAATGGC
Lif-R	GGAAGTCTGTCATGTTAGGCGC
Lta-F	AGCCCATCCACTCCCTCAGAAG
Lta-R	TGCTCTCCAGAGCAGTGAGTTC
Vegfa-F	CTGCTGTAACGATGAAGCCCTG
Vegfa-R	GCTGTAGGAAGCTCATCTCTCC
Ccr7-F	AGAGGCTCAAGACCATGACGGA
Ccr7-R	TCCAGGACTTGGCTTCGCTGTA
CD40-F	ACCAGCAAGGATTGCGAGGCAT
CD40-R	GGATGACAGACGGTATCAGTGG
IL-4-F	ATCATCGGCATTTTGAACGAGGTC
IL-4-R	ACCTTGGAAGCCCTACAGACGA
IL-5-F	GATGAGGCTTCCTGTCCCTACT
IL-5-R	TGACAGGTTTTGGAATAGCATTTCC
Ccl4-F	ACCCTCCCACTTCCTGCTGTTT
Ccl4-R	CTGTCTGCCTCTTTTGGTCAGG
Ifng-F	CAGCAACAGCAAGGCGAAAAAGG
Ifng-R	TTTCCGCTTCCTGAGGCTGGAT
IL-9-F	TCCACCGTCAAAATGCAGCTGC
IL-9-R	CCGATGGAAAACAGGCAAGAGTC
IL-10-F	CGGGAAGACAATAACTGCACCC

IL-10-R	CGGTTAGCAGTATGTTGTCCAGC
IL-21-F	GCCTCCTGATTAGACTTCGTCAC
IL-21-R	CAGGCAAAAGCTGCATGCTCAC
IL-21r-F	CACTGACTACCTCTGGACCATC
IL-21r-R	GCAGAAGGTCTCTTGGTCCTGA

1. Gao, N., et al., *Dendritic cell-epithelium interplay is a determinant factor for corneal epithelial wound repair.* Am J Pathol, 2011. **179**(5): p. 2243-53.